A Kinetic Molecular Model of the Reversible Unfolding and Refolding of Titin Under Force Extension

Bo Zhang, Guangzhao Xu, and John Spencer Evans
Laboratory for Chemical Physics, Department of Chemistry, New York University, New York, NY 10010 USA

ABSTRACT Molecular elasticity is a physicomechanical property that is associated with a select number of polypeptides and proteins, such as the giant muscle protein, titin, and the extracellular matrix protein, tenascin. Both proteins have been the subject of atomic force microscopy (AFM), laser tweezer, and other in vitro methods for examining the effects of force extension on the globular (FNIII/Ig-like) domains that comprise each protein. In this report we present a time-dependent method for simulating AFM force extension and its effect on FNIII/Ig domain unfolding and refolding. This method treats the unfolding and refolding process as a standard three-state protein folding model ($U \rightleftarrows T \rightleftarrows F$, where U is the unfolded state, T is the transition or intermediate state, and F is the fully folded state), and integrates this approach within the wormlike chain (WLC) concept. We simulated the effect of AFM tip extension on a hypothetical titin molecule comprised of 30 globular domains (Ig or FNIII) and 25% Pro-Glu-Val-Lys (PEVK) content, and analyzed the unfolding and refolding processes as a function of AFM tip extension, extension rate, and variation in PEVK content. In general, we find that the use of a three-state protein-folding kinetic-based model and the implicit inclusion of PEVK domains can accurately reproduce the experimental force-extension curves observed for both titin and tenascin proteins. Furthermore, our simulation data indicate that PEVK domains exhibit extensibility behavior, assist in the unfolding and refolding of FNIII/Ig domains in the titin molecule, and act as a force "buffer" for the FNIII/Ig domains, particularly at low and moderate extension forces.

INTRODUCTION

Elasticity is a physicomechanical property that is associated with a select number of polypeptides and proteins. Prime examples include titin (connectin), a 3.5 MD protein that spans the half-sarcomere in skeletal and cardiac muscles (Erickson, 1997; Gautel and Goulding, 1996; Higgins et al., 1994; Horowits et al., 1986, 1989; Keller, 1997; Politou et al., 1995; Rief et al., 1997), and tenascin, an extracellular matrix protein involved in cell adhesion and cell-cell mechanical interactions; (Chiquet-Ehrismann, 1995; Clark et al., 1997; Erickson, 1993; Oberhauser et al., 1998). What is common to both proteins are unique molecular aspects (e.g., secondary and tertiary structure), which convey elastic properties. In the case of titin, the elasticity derives from the reversible unfolding of ~70 folded immunoglobulin C2 (Ig) and fibronectin type III (FNIII) domains that comprise the protein (Erickson, 1994; Higgins et al., 1994; Labeit et al., 1992; Kellermayer et al., 1997; Keller, 1997; Rief et al., 1997) and, from the semistable springlike Pro-Glu-Val-Lys (PEVK)-rich domain (Rief et al., 1997; Kellermayer et al., 1997; Linke, 1996). It is believed that the tandem Ig chain acts as an extensible chain that resists stretching at longer sarcomere lengths and higher forces, whereas the PEVK region is extended under lower forces (Rief et al., 1997; Linke and Granzier, 1998) and behaves like a relatively stiff spring (Trombitas et al., 1998). Tenascins are comprised of disulfide-linked hexamer subunits, and each tenascin subunit consists of a series of repeated structural domains, which include FNIII and tandemly linked EGF-like repeats (Erickson, 1994; Chiquet-Ehrismann, 1995). In tenascins, the FNIII domains act as extensible shock absorbers with hysteresis (Oberhauser et al., 1998).

Because proteins acquire their unique functions via specific tertiary folding, then elastic behavior must be linked to protein folding of important domains. In the case of titin and tenascin, the elastic properties of both proteins are conveyed by the unfolding and refolding of individual Ig and FNIII protein domains, both of which are arranged as seven-stranded beta barrels (Potts and Campbell, 1996; Rief et al., 1997; Kellermayer et al., 1997; Oberhauser et al., 1998). The FNIII and Ig domains of titin exhibit different behavior under extension forces: FNIII exhibit 20% lower unfolding forces than Ig domains (Rief et al., 1998). AFM studies of recombinant titin molecules indicate that the forces required to unfold individual Ig domains ranged from 150 to 300 pN; the extension curves for both native and recombinant titin molecules feature "sawtooth" force patterns that reflect the successive unraveling of individual domains within the protein molecule (Rief et al., 1997, 1998). The sawtooth force-extension pattern was also observed in AFM force-extension studies of recombinant tenascin-C fragments composed of 7 or 15 FNIII domains (Oberhauser et al., 1998). "Steered" molecular dynamics studies have revealed that the unfolding of Ig domains under force gives rise to a force peak; this peak corresponds to an initial burst of backbone hydrogen bond dissociation between antiparallel β-strand A and B and between β-parallel strands A′ and G (Lu et al., 1998). What is intriguing about both titin and tenascin force extension experiments is that sequential unfolding is ob-

Received for publication 25 February 1999 and in final form 7 June 1999.
Address reprint requests to Dr. John Spencer Evans, Laboratory for Chemical Physics, Division of Basic Sciences, New York University, 345 E. 24th St., Room 1007, New York, NY 10010. Tel.: 212-998-9605; Fax: 212-995-4087; E-mail: jse@dave-edmunds.dental.nyu.edu.

0006-3495/99/09/1306/10 $2.00

served under force, but the refolding phase is nonsequential, and does not initiate until the protein molecule is extensively retracted (Rief et al., 1997, 1998; Linke et al., 1998a; Kellermayer et al., 1997; Oberhauser et al., 1998).

The behavior and function of the nonglobular PEVK domains in titin are somewhat unresolved. Trombitas and co-workers suggest that the PEVK domains in titin are permanently unfolded, nonglobular domains that function like a stiff spring (Trombitas et al., 1998). However, other experiments have demonstrated that the PEVK-rich regions, which may exist as folded species, are the major contributors to titin elasticity at low or moderate extension forces (Linke et al., 1998b; Tskhovrebova and Trinick, 1997). Furthermore, Linke and co-workers (1998b) have demonstrated that PEVK domains have entropic elasticity properties at low stretch, but that enthalpic factors (i.e., ionic strength, pH) may dominate at higher extension.

This report describes a kinetic model for folding and refolding of individual globular domains within a hypothetical titin molecule. The rationale for developing this model was inspired by the entropic spring-based wormlike chain (WLC) model (Flory, 1969), which was successfully implemented as a simulation tool for modeling titin force extension curves (Rief et al., 1997, 1998; Kellermayer et al., 1997; Linke et al., 1998a, b), and tenascin FNIII and titin Ig domain unfolding (Oberhauser et al., 1998; Rief et al., 1998). We were interested in developing a folding-refolding model for elastic protein force-extension and relaxation for the following reasons: 1) to explain the stepwise unfolding of titin and tenascin FNIII/Ig domains and the sawtooth force pattern associated with this unfolding; 2) to determine the relationship between passive force and the extension rate; 3) to determine the effect of extension on the refolding of the FNIII and Ig domains, as well as the refolding rates under different extension forces; and 4) to establish what effect, if any, PEVK domains have on the force extension process in the titin molecule.

To accomplish these goals, we applied a simple protein folding three-state model (Chan and Dill, 1994; Kuwajima, 1989; Fersht, 1993; Jaenicke, 1991; Gulukota and Wolynes, 1994; Amara and Straub, 1995; Kemmink and Creighton, 1995) to describe the unfolding and refolding of either FNIII or Ig domains under extension. We then integrated this kinetic model within the WLC concept. The consecutive unfolding and refolding of domains within a single protein molecule is modeled as a chain propagation reaction. This approach differs from previous WLC-based simulations (Oberhauser et al., 1998; Linke et al., 1998a; Rief et al., 1998), in that kinetics of unfolding and refolding are explicitly expressed, and the concentration of unfolded, intermediate, and refolding species are computed dynamically, instead of by a Monte Carlo-based probability. As shown by our data, our model can accurately reproduce the AFM and laser tweezer force-extension data for titin molecules. In addition, our findings indicate that the PEVK domains act as extensible species, and are responsible for extension under low force, in agreement with experimental observations (Linke et al., 1998b; Gautel and Goulding, 1996; Rief et al., 1997; Linke and Granzier, 1998).

METHODOLOGY

In the following sections we will discuss the development of our kinetic model for extensible protein unfolding and refolding. In the first section we will define the three-state model and the rate constants for the reversible folding and unfolding steps for a single globular protein domain. In the second section we expand the folding/refolding concept to include linearly arranged multiple globular domains, as found in titin and tenascin proteins. In the third section we adopt the WLC model (Flory, 1969; Bustamante et al., 1994) to determine the kinetics of unfolding and refolding of linearly arranged multiple globular domains within a single titin molecule. Finally, in the fourth and fifth sections we outline the procedure for simulating AFM tip force extension studies of linearly arranged multiple globular domains in a titin molecule that contains varying percentages of PEVK domains.

Kinetics and energetics of single Ig or FNIII domain unfolding and refolding

The basic premise of our three-state model is the following: for a given stretched, unfolded globular domain to refold to its original length, the domain has to overcome the energy barrier induced by the extension force. Thus, refolding of a single domain, be it Ig or FNIII, can be viewed as a two-step process: first, relaxation, i.e., recovery of length; second, stretch-free folding. The states involved are the unfolded (U), intermediate or transition (T), and fully folded (F) (Fig. 1). To model this process we must make a number of assumptions, which are based upon the experimental and theoretical information available for the titin (Rief et al., 1997, 1998; Linke

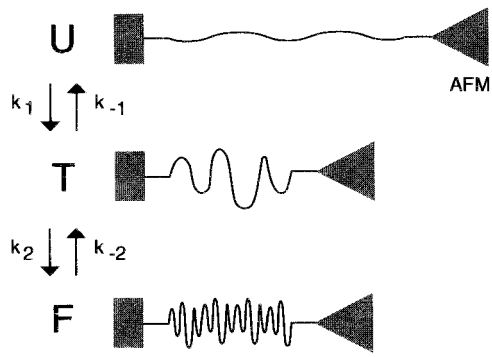

FIGURE 1 Basic protein folding model for a single FNIII/Ig domain unfolding and refolding under AFM tip force extension. A description of each state and the overall kinetic scheme is described in the Methods section. The rectangle represents the surface to which the FNIII or Ig domain attaches; the triangle represents the tip of the AFM cantilever that moves perpendicular to the surface. In "U," the FNIII/Ig domain is unfolded into an extended form by displacement of the AFM tip away from the surface. In "T," the AFM tip is retracted toward the surface, leading to a recovery in FNIII/Ig domain length. This length recovery results in a partially condensed state, "T," which has a molecular density greater than that of the "U" state. However, the "U" state does not possess correct tertiary interactions (i.e, hydrogen bonding, hydrophobic, and electrostatic interactions) or the molecular density of the fully folded state, "F." The "F" state is achieved after the formation of the "T" state, and results from reorganization and further structural condensation. Each transition is considered reversible, and the forward (folding) and reverse (unfolding) steps for each transition are characterized by rate constants.

et al., 1998a, b; Kellermeyer et al., 1997; Lu et al., 1998) and tenascin (Oberhauser et al., 1998) protein molecules (Fig. 1):

1. In the "U" state, a single Ig or FNIII domain is entirely extended by the displacement of the AFM tip, with the applied extension force evenly distributed along the chain (Fig. 1). This is considered an "unfolded" state with no tertiary interactions;
2. For the "T" state, the AFM tip has been brought closer to the surface, such that there is no longer any extension force applied to the single domain. In this instance, the partially unfolded or "U" state has recovered a portion of its original length, and exists in a condensed state that is not completely organized or ordered as compared with the fully folded state, "F" (Fig. 1). This partially folded or condensed state is analogous to the partially condensed state described in polymer and polypeptide lattice simulations (Chan and Dill, 1989, 1991, 1994; Lau and Dill, 1989). Here, the molecule lacks long-range ordering and contacts, such as tertiary interactions, and has not yet achieved the correct packing density. In the titin molecule, this transition state corresponds to the situation where coiled Ig domains are almost restored to their folded length (~3.5 nm) while the PEVK domain remains extended (Erickson, 1994). Under these conditions, there is no observable force during refolding (Kellermayer et al., 1997);
3. The "F" state corresponds to the fully folded FNIII or Ig domain (Fig. 1). In this state, the FNIII or Ig domain evolves from the "T" state through an unspecified folding pathway, and folds into the correct tertiary structure with proper molecular density. Energy release occurs upon attainment of this final ordering step, and this released energy lowers the overall energy of the system;
4. Based upon experimental observations of titin and tenascin reversible unfolding and refolding, all postulated steps are considered to be totally reversible, i.e., upon AFM tip extension, the refolded Ig or FNIII domain (state "F") will undergo extension, resulting in unfolding transitions (i.e., $F \rightarrow T$, and ultimately, $T \rightarrow U$).

We now define the transition energies. The path from T to F results in an entropy loss in the molecule. The energy difference for the transition $U \rightarrow T$ and $T \rightarrow F$ is

$$\begin{aligned} \Delta G_{U\rightarrow T} &= E_T - E_U = -T\,\Delta S_{T\rightarrow U} \\ \Delta G_{T\rightarrow F} &= E_F - E_T = -T\,\Delta S_{F\rightarrow T} \end{aligned} \tag{1}$$

Note that the free energy difference for the transition $T \rightarrow F$ ($\Delta G_{T\rightarrow F}$) is equivalent to the folding energy of a single FNIII or Ig domain, which has been experimentally determined to be ~−4 kcal/mol (Erickson, 1994).

For a single globular protein domain, the three-state folding and refolding process can be kinetically defined as:

$$U \underset{k_{-1}}{\overset{k_1}{\rightleftharpoons}} T \underset{k_{-2}}{\overset{k_2}{\rightleftharpoons}} F \tag{2}$$

where k_1 and k_2 are the forward rate constants for the $U \rightarrow T$ and $T \rightarrow F$ refolding transitions, and k_{-1} and k_{-2} are the reverse rate constants for the $F \rightarrow T$ and $T \rightarrow U$ unfolding transitions, respectively. At this juncture, we make the following assumptions:

First, since T represents a transient state, we assume that the steady-state condition applies, i.e., $d[T]/dt = 0$. Thus, the rate constants for the overall refolding (k_+) and unfolding (k_-) transitions can be expressed as a function of the individual forward (k_1, k_2) and reverse (k_{-1}, k_{-2}) rate constants, viz:

$$k_+ = \frac{k_1\,k_2}{k_{-1} + k_2} \tag{3}$$

$$k_- = \frac{k_{-1}\,k_{-2}}{k_{-1} + k_2} \tag{4}$$

Second, we assume that the transition $T \rightarrow U$ proceeds at a faster rate than $T \rightarrow F$, i.e., $k_2/k_{-1} \ll 1$. Hence, Eq. 3 can be expressed as:

$$k_+ = k_2 \exp\left(\frac{-\Delta G_{U\rightarrow T}}{kT}\right) \tag{5}$$

Because the transition $T \rightarrow F$ is a "stretch-free" folding process, the overall rate constant for this process is taken as the value of k_2, which has been experimentally determined to be ~3 s^{-1} (Kellermayer et al., 1997). In a similar manner, the overall rate constant for unfolding, k_-, can be approximated by k_{-2}.

Finally, we wish to relate the overall unfolding rate constant, k_-, to the externally applied force. AFM measurements of titin-Ig domains indicate that the unfolding distance (denoted as Δx) for this domain is 0.3 nm (Rief et al., 1997). This value has been utilized in Monte Carlo force-extension simulations of titin (Rief et al., 1997) and tenascin (Oberhauser et al., 1998). The experimentally determined unfolding rate constant (denoted as α) for tenascin-FNIII domain is 4.6×10^{-4} s^{-1} (Clarke et al., 1997). Thus, in a manner similar to the Monte Carlo simulations of titin (Rief et al., 1997) and tenascin (Oberhauser et al., 1998), we can express k_- with respect to the unfolding distance, the rate constant, and the externally applied force, f.

$$k_- = \exp(f \cdot \Delta x)\alpha \tag{6}$$

Using the WLC model to determine the energy of unfolding and refolding

Titin has been described as a molecule that acts like a molecular spring (Trinick, 1996; Erickson, 1997; Keller et al., 1997). To calculate the energy of the unfolding and folding transitions, we adopt the WLC model (Bustamante et al., 1994; Flory, 1969). A similar approach was utilized for Monte Carlo-based force extension simulations of titin (Kellermayer et al., 1997; Rief et al., 1997) and tenascin (Oberhauser et al., 1998). Briefly, the WLC model describes a molecular chain as a deformable continuum or rod of a given persistence length, A, which is a measure of the molecule's stiffness. The relationship between the end-to-end length (z) and the external force (f) are given by (Bustamante et al., 1994; Flory, 1969; Kellermayer et al., 1997; Rief et al., 1997; Oberhauser et al., 1998):

$$f = \frac{kT}{A} \cdot \left[\frac{1}{4(1 - Z/L)^2} - \frac{1}{4} + \frac{z}{L}\right] \tag{7}$$

where k is the Boltzmann constant, T is temperature, and L is contour length (i.e., the length of a fully extended WLC chain). For our calculations, $A = 0.4$ nm (Kellermayer et al., 1997; Rief et al., 1997; Oberhauser et al., 1998). In our model, we consider the unfolded portion of the FNIII/Ig domains and the PEVK domain as contributors to the WLC chain; the folded portion of the domains are excluded.

To determine the value of L to use in our simulations, we sum the contour lengths of all the Ig or FNIII domains that comprise the single protein molecule. We assume that in the fully extended chain, the contour length is proportional to the number of amino acids. To include the PEVK domain in titin, we adjust the value of L to reflect the addition of amino acid residues representing the PEVK domain (see below for further details). For titin, the inclusion of the PEVK domain results in a 25% increase in the contour length, since the PEVK domain represents ~25% of the titin sequence (Kellermayer et al., 1997; Rief et al., 1997). Using Eq. 7, the energy of force-extension refolding ($\Delta G_{U\rightarrow T}$), as given in Eq. 5, can now be re-expressed as:

$$\Delta G_{U\rightarrow T} = \int f \cdot dx \tag{8}$$

We now have an expression that relates the displacement, extension force, and the refolding energy for the $U \rightarrow T$ transition.

Kinetics of multiple domain unfolding and refolding

Realistically, force extension and relaxation behavior in titin and tenascin molecules reflect the unfolding/refolding of multiple, linearly arranged domains in a single molecule. If we consider a single titin or tenascin molecule to be comprised of N domains, we can express the overall refolding kinetics of the entire protein as:

$$F_0 \underset{k_{10}}{\overset{k_{01}}{\rightleftarrows}} F_1 \underset{k_{21}}{\overset{k_{12}}{\rightleftarrows}} F_2 \ldots \underset{k_{\mathrm{n,\,n-1}}}{\overset{k_{\mathrm{n-1,\,n}}}{\rightleftarrows}} \ldots F_{\mathrm{N}} \tag{9}$$

where F_{n} represents the species that have n of N domains in the folded state, and $k_{\mathrm{n-1,n}}$, $k_{\mathrm{n,n-1}}$ denote the rate constants for the forward and reverse transitions involving $F_{\mathrm{n-1}}$ to F_{n}, respectively. The rate constants for the overall forward (k_+) and reverse (k_-) transitions thus become

$$k_{\mathrm{n-1,\,n}} = (n-1)\,k_+ \tag{10}$$

$$k_{\mathrm{n,\,n-1}} = (N-n)\,k_- \tag{11}$$

We will now construct an expression that describes the time-dependent concentration of each species that undergoes refolding. To do this, we make a simplifying assumption that each species unfolds and refolds independently of one another, i.e., a non-cooperative case. The concentration, C_{i}, of any species F_{i} as a function of time must satisfy the following ordinary differential equation set:

$$\frac{dC_{\mathrm{i}}(t)}{dt} = \sum_{\mathrm{j}=1}^{\mathrm{N}} \left(C_{\mathrm{j}}(t)\,k_{\mathrm{ji}} - C_{\mathrm{i}}(t)\,k_{\mathrm{ij}}\right) \tag{12}$$

where

$$i = 0, 1, \ldots, N$$

for all i, j. Note that i, j are measurable states. For Eq. 12, equilibrium conditions apply. The boundary conditions for this set are:

$$C_{\mathrm{i}}^{\mathrm{t}=0} = C_{\mathrm{i}}^{\mathrm{ini}} \tag{13}$$

$$C_{\mathrm{i}}^{\mathrm{t}=\infty} = C_{\mathrm{i}}^{\mathrm{eq}} \tag{14}$$

where $C_{\mathrm{i}}^{\mathrm{ini}}$ and $C_{\mathrm{i}}^{\mathrm{eq}}$ are the concentrations of each species at $t = 0$ and at equilibrium, respectively. A general solution for Eq. 12 is given by Rodiguin and Rodiguina, 1964:

$$C_{\mathrm{i}}(t) = C_{\mathrm{i}}^{\mathrm{eq}} + \sum_{\mathrm{s}=1}^{\mathrm{N}} a_{\mathrm{is}} \exp(-\lambda_{\mathrm{s}} t) \tag{15}$$

For all i, s. Here, s refers to the eigenstates. The n values of λ_{s} can be obtained via the solution to the eigenvalue matrix:

$$\begin{vmatrix} \lambda - \sum k_{0\mathrm{j}} & k_{10} & k_{20} & \ldots & k_{\mathrm{N0}} \\ k_{01} & \lambda - \sum k_{1\mathrm{j}} & k_{21} & \ldots & k_{\mathrm{N1}} \\ k_{02} & k_{12} & \lambda - \sum k_{2\mathrm{j}} & \ldots & k_{\mathrm{N2}} \\ \vdots & \ldots & \ldots & \ldots & \vdots \\ k_{0\mathrm{N}} & k_{1\mathrm{N}} & k_{2\mathrm{N}} & \ldots & \lambda - \sum k_{\mathrm{Nj}} \end{vmatrix} = 0 \tag{16}$$

and a_{is} are the solutions of the following equations:

$$a_{\mathrm{is}}\lambda_{\mathrm{s}} + \sum_{\mathrm{j}=0}^{\mathrm{N}} k_{\mathrm{ji}} a_{\mathrm{js}} - \left(\sum_{\mathrm{j}=0}^{\mathrm{N}} k_{\mathrm{ij}}\right) a_{\mathrm{is}} = 0 \tag{17}$$

$$\sum_{\mathrm{s}=1}^{\mathrm{N}} a_{\mathrm{is}} = C_{\mathrm{i}}^{0} - C_{\mathrm{i}}^{\mathrm{eq}} \tag{18}$$

$$\sum_{\mathrm{i}=0}^{\mathrm{N}} a_{\mathrm{is}} = 0 \tag{19}$$

for all i, s. Note the following: 1) Eq. 17 is obtained by substituting Eq. 15 into Eq. 12; 2) Eq. 12, for $t = 0$, yields Eq. 18; 3) Eq. 19 is the condition satisfied by a unimolecular process, i.e., conservation of the total concentration.

Once $C_{\mathrm{i}}^{\mathrm{t}}$ terms are calculated, we can obtain the concentration distribution of all species, i, for a period of time, t, which corresponds to a specific extension during the simulation of the AFM force-extension experiments. From the concentration distribution, we obtain the average number of folded domains, N:

$$N(t) = \sum i \cdot C_{\mathrm{i}}^{\mathrm{t}} \tag{20}$$

and the average force, F:

$$F(t) = \sum f_{\mathrm{i}} \cdot C_{\mathrm{i}}^{\mathrm{t}} \tag{21}$$

for $i = 0, 1, \ldots N$, where f_{i} is the distributed force in i.

Simulation of the unfolding/refolding cycle: constant extension rate

Our goal is to simulate an AFM force extension experiment, wherein a titin molecule comprised of 30 FNIII (or Ig) domains plus the PEVK domain experiences extension and relaxation. For a cycle of unfolding and refolding, we assume a constant pulling/releasing speed of the AFM tip. Thus, each cycle will have a duration, T,

$$T = 2\left[\frac{(L_{\max} - L_{\min})}{V}\right] \tag{22}$$

where $L_{\max}$ and $L_{\min}$ are the maximum and minimum contour lengths, respectively, and V is the pulling-releasing velocity. During the simulated AFM extension-retraction process, the end-to-end length changes constantly over time. Thus, the values of K, λ, and a are time-dependent (note that Eq. 15 specifies the situation of constant end-to-end length, where the values of K, λ, and a are time-independent).

To overcome the impracticality of a continuous time simulation, we developed a discrete time scheme to approximate the unfolding-refolding simulation. The AFM extension-retraction simulations utilized the following scheme:

1. The cycle period is partitioned into an M grid lattice, with $\Delta t = T/M$. At a lattice point we have $t_{\mathrm{m}} = m^* \Delta t$, and $L_{\mathrm{m}} = L_{\min} + t_{\mathrm{m}}{}^* V$. The values of K and λ are calculated accordingly;
2. During the time interval from t_{m} to $t_{\mathrm{m+1}}$, the end-to-end length is assumed to be invariant; hence, Eq. 15 is used to calculate the concentration $C_{\mathrm{i}}(t)$, for $t_{\mathrm{m}} < t_{\mathrm{m+1}}$. Similarly, Eqs. 20 and 21 were used to calculate average number of folded domains and force, respectively;
3. The values for $C_{\mathrm{i}}(t)$ at $t = t_{\mathrm{m+1}}$ obtained in (2), above, are used as the values for C_{i}^{0} (Eq. 18) for the next period, i.e., $t_{\mathrm{m+1}}$ to $t_{\mathrm{m+2}}$. At $t = 0$, all the domains are assumed to exist in the fully folded state.

Assuming that the time step Δt is sufficiently small, this discrete time scheme can simulate the continuous time process with satisfactory accuracy.

Simulation of the refolding cycle: PEVK content

To learn more about how PEVK responds to AFM tip force, we simulated AFM tip force extension of titin molecules containing varying percentages of PEVK domains in the presence of a fixed number of Ig domains. To perform this type of AFM tip simulation, we make the assumption that the persistence length of a PEVK domain is equivalent to that of an Ig globular domain. Basically, we treat PEVK as part of the entropic spring model with the same elastic properties as the FNIII/Ig domains. So, when we consider the contour length of the titin molecule, we add the maximum spacing length of the PEVK part to the overall titin contour length. Hence, the contour length becomes the parameter that represents PEVK content. One does not need to adjust other simulation parameters to account for the inclusion of PEVK. The AFM force extension simulation begins with titin molecule extension, followed by chain relaxation and observation of domain folding as a function of time. The simulation is repeated, only now the contour length of the chain is varied by a fixed amount to represent the inclusion of additional PEVK domains (see above). By varying the contour length and repeating the simulation, we can examine the effects of extension and PEVK content on the refolding rate.

RESULTS

In this paper, a chain comprised of 30 globular domains (e.g., FNIII, Ig) and a discrete PEVK content is utilized as a model of the titin molecule. Since we assume that the unfolding and refolding transitions for a given domain are non-cooperative, the results obtained for this chain model, could, in theory, apply to other protein molecules of any defined length. Our parameters for simulating AFM unfolding and refolding phenomena utilized the following data: 1) all FNIII or Ig domains within the chain are considered equivalent, and a total number of 30 domains comprises each chain; 2) each FNIII or Ig domain has a fully extended length (L) of 31 nm and a folded length of 3.5 nm; 3) A = 0.4 nm; 4) each FNIII or Ig domain has stretch-free folding and unfolding rate constants of 3 s^{-1} and 4.6×10^{-4} s^{-1}, respectively; 5) all simulations were conducted for $T = 300$ K; and 6) all simulations, with the exception of those presented in Fig. 5 A and B assume a PEVK content of 25% (i.e., contour length = 225 nm) of the total chain length.

The effect of extension rate on domain unfolding and refolding

We first examine the effects of AFM tip extension rate on domain refolding. As shown in Fig. 2, the extension rate has a pronounced effect on the refolding phase. The typical cycle involves an unfolding phase, which commences with applied tension and continues up to a specified AFM tip displacement (i.e., 820 nm). Note that the fully extended length for a 30-domain chain is 930 nm. With the release of the extension force, the refolding phase is initiated. This phase continues up to the theoretical fully relaxed length (i.e, 121 nm). Several interesting observations were noted in these simulations. First, the typical "sawtooth" force-extension unfolding curves that were observed in AFM (Rief et al., 1997, 1998; Oberhauser et al., 1998) and laser-tweezer (Kellermayer et al., 1997) force extension studies were replicated by our simulation (Fig. 2). These "sawtooth"

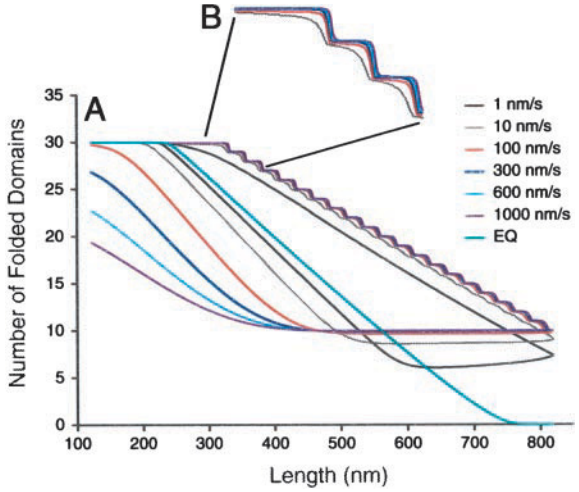

FIGURE 2 Simulation of unfolding and refolding events in a single titin molecule as a function of AFM tip extension. Each color-coded curve represents a different AFM tip extension rate, plotted as a function of FNIII/Ig folded domain number and AFM tip-to-surface distance. (A) Main graph; (B) expansion of indicated region shown in (A). Extension rates of 1, 10, 100, 300, 600, and 1000 nm/s are plotted, along with the equilibrium state. For comparison with experimental data, see the following references and the original figures noted therein: Rief et al., 1997 (Figs. 1 and 3), 1998 (Fig. 4); Oberhauser et al., 1998 (Fig. 1) Kellermayer et al., 1997 (Fig. 3 A).

patterns were more pronounced for simulated extension rates $\geq$ 10 nm/s. Second, as extension rate increases, the overlap between unfolding and refolding curves decreases. As seen in the early stages of force release, there is a "plateau" phase (i.e., slope = 0). This "plateau" phase indicates that there is no change in the average number of folded domains (Fig. 1); i.e., there is no domain refolding, presumably due to excessive extension. According to the experiments conducted by Rief and colleagues (1997), the refolding phase commences at low extension, i.e., the end-to-end length is less than one-half of its fully extended length. Assuming that the fully extended length is 930 nm, we find that our simulations generate the same data for extension rates $\geq$100 nm/s (Fig. 2).

In Fig. 3 A we examine in more detail the typical "sawtooth" force-extension pattern for a hypothetical 30 Ig domain titin molecule. Here, the distance between each force peak corresponds to an approximate displacement value of 25 nm, which is similar to the contour length of a single FNIII or Ig domain (Rief et al., 1997, 1998; Oberhauser et al., 1998; Kellermayer et al., 1997). Moreover, as chain extension progresses, there is a corresponding increase in the force required to unfold each successive domain in the chain. Collectively, these observations correspond to the experimental results obtained by force-extension experiments (Rief et al., 1997; Oberhauser et al., 1998; Kellermayer et al., 1997). In this same figure one should note the direct relationship between extension rate and peak amplitude. One explanation for this phenomenon is the following. If the extension rate is fast, then during the extension or unfolding phase the AFM extension force has insufficient

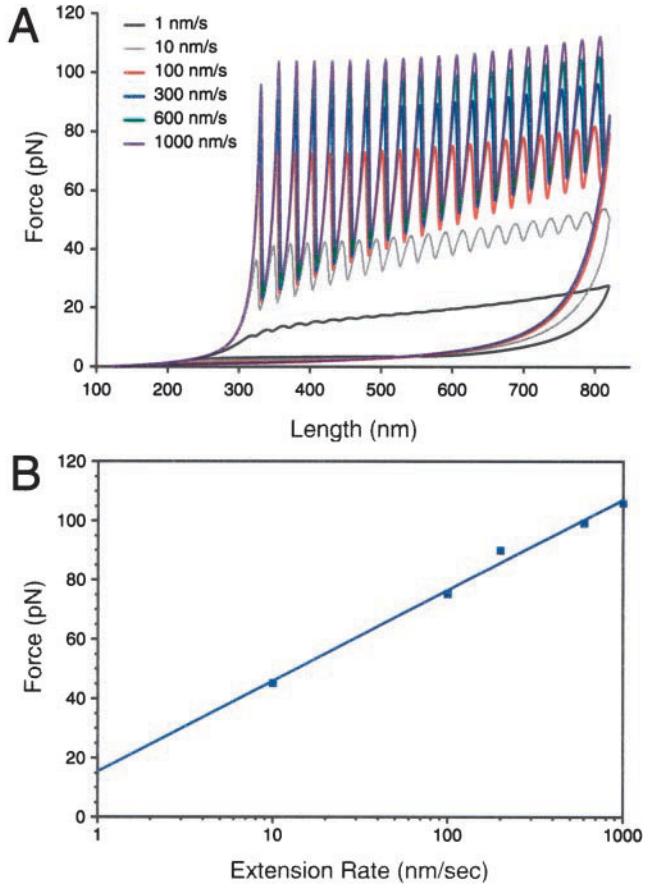

FIGURE 3 (*A*) Extension rate-dependent simulation of applied AFM force for a titin molecule. Extension rates are given in the figure. For comparison with experimental data, see the following references: Rief et al., 1997 (Figs. 1 and 3), 1998 (Fig. 4); Oberhauser et al., 1998 (Fig. 1) Kellermayer et al., 1997 (Fig. 3 *A*). (*B*) Simulated extension rate-extension force curve (x-axis semilog) for an FNIII/Ig-like chain. For comparison with experimental data, see the following references and the original figures noted therein: Rief et al., 1997 (Fig. 5), 1998 (Fig. 7); Oberhauser et al., 1998 (Fig. 3 *B*).

time to propagate through the chain. This leads to very abrupt unfolding transitions, with characteristic "steep" sawtooth curves and increased force amplitudes (Fig. 3 *A*). During the refolding phase, as the extension rate increases, the extended chain is unable to relax sufficiently, which, in turn, results in incomplete refolding. The opposite situation occurs with slower extension rates (Figs. 2 and 3 *A*). For the extreme case where the extension rate is very slow (Fig. 2, the equilibrium curve), each step of unfolding and refolding is at equilibrium. In this situation, it can be clearly seen that the AFM extension force can propagate throughout the entire chain evenly, which leads to complete unfolding and refolding. Under these conditions, the typical force-extension "sawtooth" pattern is not observed, since the extension force propagates evenly as a function of time. In other words, we cannot detect any abrupt changes at the AFM tip. As shown elsewhere, the applied AFM extension force exhibits a logarithmic relationship to extension rate (Rief et al., 1997, 1998; Kellermayer et al., 1997). As shown in Fig. 3 *B*, this is also observed in our simulation data.

The relationship between applied force and domain unfolding

An important observation was noted when extension force and the average number of folded domains were compared as a function of extension length (Fig. 4). Here, each force peak of the "sawtooth" force extension curve (*black line*) was found to align with a peak corresponding to the unfolding of a single Ig domain (*gray line*). One explanation for this correlation can be conceptualized in the following manner. At the macroscopic level, as the molecular chain becomes progressively extended, the average extension force that is required to extend the chain must increase due to the springlike character of the chain. However, at the microscopic level, the extension force undergoes a cyclical increase and decrease in value as each Ig domain undergoes unfolding. An individual Ig domain will unfold only when the external force is sufficiently high; hence, we observe an initial increase in force at the AFM tip. Subsequently, when a given domain becomes unfolded, the applied force is redistributed throughout the chain so that the force at the AFM tip decreases; hence, we observe a decrease in the force curve at that interval. Simultaneous to the decrease in AFM tip force is the decrease in the average folded domain number (by 1). These findings are in agreement with experimental observations that the Ig or FNIII domains of titin and tenascin undergo sequential unfolding in response to external force, and that the unfolding of individual domains results in the relaxation of tension within the molecule (Rief et al., 1997, 1998; Oberhauser et al., 1998).

The effect of PEVK domains on the unfolding and refolding of Ig domains

Previous studies have indicated that the titin-specific PEVK-rich domain functions as a semistable entropic

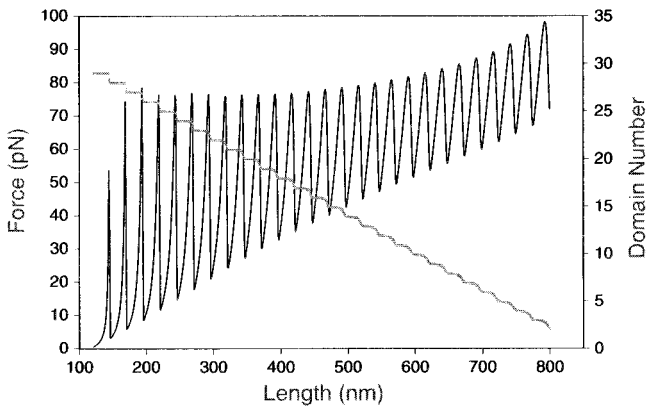

FIGURE 4 Simulation of AFM tip extension as a function of FNIII/Ig domain unfolding. Here, each force peak (*black curve*) is plotted along with the number of folded domains (*gray curve*) as a function of AFM tip extension. For these simulations, extension rate = 100 nm/s.

spring that extends under low force (Rief et al., 1997; Kellermayer et al., 1997; Tskhovrebova and Trinick, 1997; Linke, 1996). Recent data suggest that PEVK stiffness properties arise from electrostatic and hydrophobic interactions within the PEVK segment (Linke et al., 1998b; Linke and Granzier, 1998). To determine what effect the PEVK-rich domain has on the Ig domain unfolding and refolding process, we varied the content of PEVK domains within the hypothetical titin molecule. As shown in Fig. 5 *A*, two phenomena are observed. First, the hypothetical titin molecule requires more extension to elicit a force peak as the PEVK content rises. This implies that the PEVK regions are exhibiting extensible behavior to some degree. This finding is in agreement with experimental studies showing that PEVK domains, and not Ig or FNIII domains, extend under low or moderate extension forces (Gautel and Goulding, 1996; Kellermayer et al., 1997; Linke et al., 1998a, b). Second, as the titin molecule reaches the hypothetical extension limit, the applied force required for extension is observed to increase as a function of PEVK content. These results are consistent with the notion that the PEVK domain acts as a force "buffer" (Trombitas et al., 1998; Linke et al., 1998b; Linke and Granzier, 1998), i.e., force distribution occurs within the PEVK domain in addition to the rest of the FNIII/Ig-containing chain.

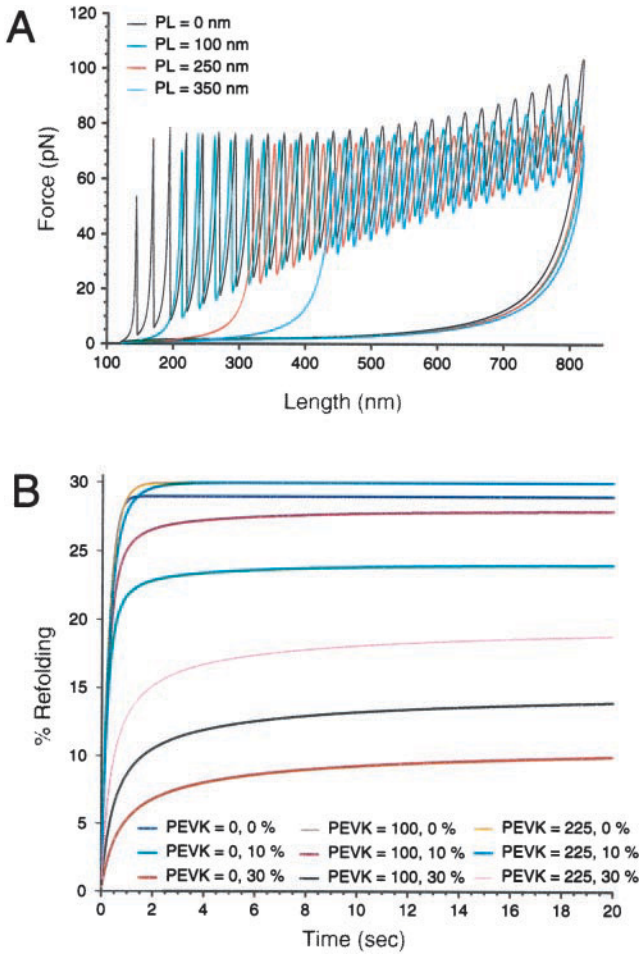

FIGURE 5 (*A*) The effect of PEVK content on the simulation of applied AFM force for a titin molecule. PL = PEVK contour length, which represents a conversion from the PEVK percentage in the chain, i.e., 0 nm = 0%, 100 nm = 10%, and so on. For these simulations, extension rate = 100 nm/s; (*B*) Time-dependent simulations of the AFM tip extension experiment for a titin molecule as a function of PEVK content. These simulations examine the refolding of the titin molecule as a function of time after AFM tip release. Each curve represents a different PEVK content (expressed in nm) and different AFM tip extension or stretch (expressed in percent of total chain length).

The PEVK content also has an effect on the refolding phase of the titin molecule (Fig. 5 *B*). In this simulation, we are examining the effects that PEVK content and AFM tip extension have on refolding rates. Note that a significant percentage of titin refolding occurs within the first second, indicating that the rate constant for refolding, regardless of PEVK content, is $\approx 1\ s^{-1}$. This refolding rate is consistent with the experimentally determined FNIII/Ig domain refolding rates (Erickson, 1994). An analysis of the refolding curves reveals that, in the absence of extension force, Ig domain refolding proceeds to completion regardless of PEVK content (Fig. 5 *B*). Conversely, under extension, the extent to which the titin molecule can refold is reduced. This was also observed in the Ig domain unfolding-refolding cycles (see Fig. 2). However, in this instance, the PEVK content is observed to play an important role in the refolding process. As shown in Fig. 5 *B* for 10% and 30% extension, the extent of refolding is directly related to PEVK content, i.e., the higher the PEVK content within the chain, the greater the extent of FNIII/Ig domain refolding. This can be explained by the ability of the PEVK domain to become extended under force, and to a certain degree, reduce the extension or unfolding of the FNIII/Ig domains. Clearly, our simulations indicate that PEVK domain content and extensibility play an important role in the reversible unfolding and refolding of the entire protein molecule.

DISCUSSION

The use of WLC-based simulation has assisted our understanding of how globular (FNIII/Ig) (Kellermeyer et al., 1997; Oberhauser et al., 1998; Linke et al., 1998a; Lu et al., 1998) and nonglobular (PEVK) (Trombitas et al., 1998; Linke et al., 1998b) domains behave under applied force and upon release. The present study approaches the problem of molecular elasticity using the WLC-entropic spring model, but with a novel "twist": apply a protein folding three-state model (Chan and Dill, 1994; Kuwajima, 1989; Fersht, 1993; Jaenicke, 1991; Gulukota and Wolynes, 1994; Amara and Straub, 1995; Kemmink and Creighton, 1995) and develop a domain concentration-dependent, discrete time-based simulation model that addresses the force extension-relaxation behavior of a chain consisting of 30 FNIII/Ig-like domains. The advantages of this approach are that the kinetics of unfolding and refolding are explicitly expressed, and the concentration of unfolded, intermediate, and refolded species are computed dynamically. Unlike

other WLC-based simulation studies (Oberhauser et al., 1998; Kellermayer et al., 1997; Linke et al., 1998a, b; Rief et al., 1998), our protein folding-based approach permits the examination of FNIII/Ig domain unfolding and refolding rates as a function of extension force, extension rate, and PEVK content. In addition, since titin domain unfolding in myoblasts occurs after prolonged exposure to extension force (Rief et al., 1998), a time-based simulation is an appropriate method for studying the effects of extension time on FNIII/Ig domain unfolding and recovery.

Our simulations indicate that there is a direct relationship between extension rate and FNIII/Ig domain unfolding and refolding (Figs. 2 and 3 *A*). Slow extension rates permit complete unfolding and refolding to occur, and the AFM extension force is allowed to propagate throughout the molecule evenly. These results are in agreement with experimental observations (Oberhauser et al., 1998; Kellermayer et al., 1997; Rief et al., 1997, 1998). As the extension rates increase, the unfolding and refolding processes are affected. Higher extension rates do not allow force propagation throughout the titin molecule, leading to abrupt unfolding transitions (Fig. 3 *A*). Furthermore, higher extension rates do not allow full relaxation, which leads to incomplete FNIII/Ig domain refolding (Fig. 3 *A*). Our simulations also demonstrate the relationship between "sawtooth" force extension peaks and individual FNIII/Ig domain unfolding. As shown in Fig. 4, the extension force undergoes a cyclical increase and decrease in value as each FNIII/Ig domain undergoes unfolding. Subsequently, when a given domain becomes unfolded, the applied force is redistributed throughout the titin molecule. These results support the notion that the FNIII/Ig domains experience sequential unfolding and refolding during the titin and tenascin extension-relaxation process (Lu et al., 1998; Oberhauser et al., 1998; Kellermayer et al., 1997; Rief et al., 1997, 1998).

We should caution the reader that the simulation parameters utilized in our study are derived from in vitro force-extension experiments conducted on single titin molecules (Rief et al., 1997, 1998; Kellermayer et al., 1997). These values should not be construed as being representative of titin elasticity within the context of muscle fiber extension and relaxation in vivo. As pointed out in recent immunodetection studies (Linke et al., 1998a, b), one has to assume that titin molecules do not necessarily behave as independent entities; rather, there may be other intermolecular interactions (e.g., cooperative effects) between individual titin molecules and/or between titin and other muscle proteins. These interactions could affect extension velocity, extension length, unfolding and refolding, and overall elasticity. Realistically, our simulation data provide insight into in vitro force-extension behavior and titin elasticity, but do not fully address the nature of molecular elasticity within muscle fibers in vivo.

Recent experimental evidence now supports the notion that PEVK regions play an active role in titin elasticity (Linke et al., 1998; Linke and Granzier, 1998). This is also evident from our simulation data. First, force distribution must occur within the PEVK domain in addition to the rest of the FNIII/Ig portion of the titin molecule, and more force is required to extend the molecule when PEVK is present (Fig. 5 *A*). In other words, the PEVK domains behave as entropic springs at low or moderate extension; we do not observe Ig or FNIII domain unfolding under low or moderate extension (i.e., up to 300 nm, Fig. 2). The extensibility and entropic spring behavior of PEVK under low or moderate extension are supported by experimental observations in skeletal muscle (Gautel and Goulding, 1996; Linke et al., 1998a; Linke and Granzier, 1998). Second, the PEVK content influences the refolding phase of the globular FNIII/Ig domains: the higher the PEVK content within the chain, the greater the extent of FNIII/Ig refolding. In other words, the PEVK domains enhance the relaxation and recovery of FNIII/Ig structure, particularly at high extension (Fig. 5, *A* and *B*). Our findings are supported by other studies that have demonstrated that titin Ig domain unfolding is uncommon under normal physiological forces, and does unfold under prolonged extension to prevent muscle sarcomere damage (Rief et al., 1997, 1998). Hence, we conclude that FNIII/Ig domain unfolding and refolding processes are potentially regulated by PEVK regions as a means of increasing the resistance to extension.

We address the possible existence of intermediate or partially folded state(s) for FNIII/Ig and PEVK domains during the extension and relaxation phases during AFM tip titin and tenascin pulling experiments. First, let us address the FNIII/Ig domains. To date, experiments have not yet provided information at the atomic level regarding the unfolding and refolding of a single or multiple Ig/FNIII domains within the titin chain. However, the "steered" MD simulations of Lu and co-workers have shown that a single Ig domain unfolds via a series of steps (Lu et al., 1998). One of the initial steps in unfolding leads to the existence of a partially folded but stable Ig molecule whose β-sheets have moved away from one another and whose loop regions have become extended (Lu et al., 1998). Based on this observation and the observations that globular protein folding pathways may involve the formation of one or more intermediate folded states (Chan and Dill, 1994; Kuwajima, 1989; Fersht, 1993; Jaenicke, 1991; Gulukota and Wolynes, 1994; Amara and Straub, 1995; Kemmink and Creighton, 1995), we have included a single quasi-folded or "condensed" state in our overall kinetic scheme (Fig. 1), although the MD simulations of Lu et al. suggest that a single intermediate model may be an oversimplification. Despite this potential shortcoming, the simple three-state model has reasonably reproduced many experimental features of force extension (Figs. 1–3). This would suggest that FNIII or Ig domain intermediate folding state(s) do play a role in the overall extension and relaxation processes of titin and tenascin molecules. It is apparent that FNIII or Ig unfolding and refolding processes, and the existence of intermediate folded states, becomes an important issue. For example, how do PEVK, FNIII, or Ig domain intermediate state(s) affect the relaxation or recovery of the titin and tenascin

molecules? Is there a process by which "trapping" in unfavorable intermediate states is avoided? Do PEVK domains influence the FNIII/Ig folding pathway to any extent? Clearly, further experimentation, and the development of more detailed and accurate simulation models for titin and tenascin, will address these questions.

This leads us to the issue of PEVK folding and the possibility that PEVK itself undergoes reversible unfolding and refolding during force extension. How does the structure of PEVK contribute to the elastic behavior of titin? Although the secondary and tertiary structure of the PEVK domain are not established, Trombitas et al. (1998) and Gautel and Goulding (1996) inferred from their experiments that the PEVK domain may adopt a random conformation or is permanently unfolded. However, recent experiments indicate that PEVK may exhibit enthalpic "stiffening" that translates into titin-based myofibril stiffness (Linke et al., 1998b). Presumably, complementary electrostatic interactions between Lys and Glu and hydrophobic interactions involving Val and Pro are the contributing factors that permit PEVK to behave as an elastic molecule (Linke et al., 1998b). Given that Pro residues are often located in β-turn (Xu and Evans, 1999; Dyson et al., 1988; Urry, 1982) or in polyproline type II helices (Williamson, 1994), it may be that the secondary structure of the repetitive PEVK domain is somewhat helical or coiled, and can undergo reversible unfolding and refolding in response to extension force. Clearly, experimental studies that elucidate the structure of PEVK repeats will provide a better understanding of PEVK elastic behavior.

Finally, we would like to suggest additional modifications and applications of our current model. A major advantage of our model is that it can be modified to incorporate multistep folding and the inclusion of additional transition folding states, or it can be parametrized for specific types of globular domains. As an example of the former possibility, let us consider the following. As shown by Lu and co-workers, molecular dynamics simulations of the titin Ig domain suggest that more than one intermediate partially unfolded state exists as the force extension process evolves (Lu et al., 1998). This idea could be tested by constructing an appropriate multistate model and simulating the force extension process. One could then determine whether this type of multistate model can accurately mimic force extension Ig or FNIII domain unfolding and refolding as observed in AFM experiments (Rief et al., 1997, 1998; Linke et al., 1998a; Kellermayer et al., 1997). As an example of the latter possibility, recent AFM force extension experiments conducted on Ig- and FNIII-containing titin and tenascin protein fragments indicate that titin FNIII domains exhibit 20% lower unfolding forces than titin Ig domains, but unfold at forces that are 2$\times$ greater than those observed for tenascin FNIII domains (Rief et al., 1998). These findings suggest that the transition energies for unfolding (see Eq. 1) may be different for titin FNIII, Ig, and tenascin FNIII domains. One could modify our current model to include different transition energies and rate constants for each type of domain, then proceed to simulate the force extension curves for hypothetical Ig and FNIII domains. These simulations could then be compared against existing AFM data (Rief et al., 1998). These types of applications are currently being developed.

This work was supported by the National Science Foundation (CAREER Award MCB 95-13250; MCB 98-16703), and is contribution number 8 from the Laboratory for Chemical Physics, New York University.

REFERENCES

Amara, P., and J. E. Straub. 1995. Folding model proteins using kinetic and thermodynamic annealing of the classical density function. *J. Phys. Chem.* 99:14840–14853.

Bustamante, C., J. F. Marko, E. D. Siggia, and S. Smith. 1994. Entropic elasticity of lambda phage DNA. *Science.* 265:1599–1600.

Chan, H. S., and K. A. Dill. 1989. Compact polymers. *Macromolecules.* 22:4559–4573.

Chan, H. S., and K. A. Dill. 1991. Polymer principles in protein structure and stability. *Annu. Rev. Biophys. Biophys. Chem.* 20:447–490.

Chan, H. S., and K. A. Dill. 1994. Transition states and folding dynamics of proteins and heteropolymers. *J. Chem. Phys.* 100:9238–9257.

Chiquet-Ehrismann, R. 1995. Tenascins, a growing family of extracellular matrix proteins. *Experimentia.* 51:853–862.

Clark, R., H. P. Erickson, and T. A. Springer. 1997. Tenascin supports lymphocyte rolling. *J. Cell. Biol.* 137:755–765.

Clarke, J., S. J. Hamill, and C. M. Johnson. 1997. Folding and stability of a fibronectin type III domain of human tenascin. *J. Mol. Biol.* 270: 771–778.

Dyson, H. J., M. Rance, R. A. Houghten, R. A. Lerner, and P. E. Wright. 1988. Folding of immunogenic peptide fragments of proteins in water solution. I. Sequence requirements for the formation of a reverse turn. *J. Mol. Biol.* 201:161–200.

Erickson, H. P. 1993. Tenascin-C, tenascin-R, and tenascin-X: a family of talented proteins in search of functions. *Curr. Opin. Cell. Biol.* 5:869–876.

Erickson, H. P. 1994. Reversible unfolding of fibronectin type III and immunoglobulin domains provides the structural basis for stretch and elasticity for titin and fibronectin. *Proc. Natl. Acad. Sci. USA.* 91: 10114–10118.

Erickson, H. P. 1997. Stretching single protein molecule: titin is a wield spring. *Science.* 276:1090–1091.

Fersht, A. R. 1993. Protein folding and stability: the pathway of folding of barnase. *FEBS Lett.* 325:5–16.

Flory, P. J. 1969. The statistical distribution of configuration. *In* Statistical Mechanics of Chain Molecules. Wiley Interscience, New York.

Fong, S., S. J. Hamill, M. Proctor, S. M. Freund, G. M. Benian, C. Chothia, M. Bycroft, and J. Clarke. 1996. Structure and stability of an immunoglobulin superfamily domain from tuitchin, a muscle protein of the nematode *Caenorhabditis elegans. J. Mol. Biol.* 264:624–639.

Gautel, M., and D. Goulding. 1996. A molecular map of titin/connectin elasticity reveals two different mechanisms acting in series. *FEBS Lett.* 385:11–14.

Gulukota, K., and P. G. Wolnyes. 1994. Statistical mechanics of kinetic proofreading in protein folding. *Proc. Natl. Acad. Sci. USA.* 91: 9292–9296.

Hayashi, C. Y., and R. V. Lewis. 1998. Evidence from flagelliform silk cDNA for the structural basis of elasticity and modular nature of spider silks. *J. Mol. Biol.* 275:773–784.

Higgins, D. G., S. Labeit, M. Gautel, and T. J. Gibson. 1994. The evolution of titin and related giant muscle proteins. *J. Mol. Evol.* 38:395–404.

Horowits, R., E. S. Kempner, M. E. Bisher, and R. J. Podolsky. 1986. A physiological role for titin and nebulin in skeletal muscle. *Nature (Lond.).* 323:160–164.

Horowits, R., K. Maruyama, and R. J. Podolsky. 1989. Elastic behavior of connectin filament during thick filament movement in activated skeletal muscle. *J. Cell Biol.* 109:2169–2176.

Jaenicke, R. 1991. Protein folding: Local structures, domains, subunits, and assemblies. *Biochemistry.* 30:3147–3160.

Keller, T. C. S. 1997. Molecular bungees. *Nature.* 387:233–235.

Kellermayer, M. S. Z., and H. L. Granzier. 1996. Elastic properties of single titin molecules made visible through fluorescent F-actin binding. *Biochem. Biophys. Res. Commun.* 221:491–497.

Kellermayer, M. S. Z., S. B. Smith, H. L. Granzier, and C. Bustamante. 1997. Folding-unfolding transitions in single titin molecules characterized with lazer tweezers. *Science.* 276:1112–1116.

Kemmink, J., and T. E. Creighton. 1995. The physical properties of local interactions of tyrosine residues in peptides and unfolded proteins. *J. Mol. Biol.* 245:251–260.

Kuwajima, K. 1989. The molten globule state as a clue for understanding the folding and cooperativity of globular-protein structure. *Proteins: Struct. Funct. Genet.* 6:87–103.

Labeit, S., M. Gautel, A. Lakey, and J. Trinick. 1992. Towards a molecular understanding of titin. *EMBO J.* 11:1711–1716.

Lau, K. F., and K. A. Dill. 1989. A lattice statistical mechanics model of the conformational and sequence spaces of proteins. *Macromolecules.* 22:3986–3997.

Linke, W. A. 1996. Towards a molecular understanding of the elasticity of titin. *J. Mol. Biol.* 261:62–71.

Linke, W. A., and H. Granzier. 1998. A spring tale: new facts on titin elasticity. *Biophys. J.* 75:2613–2614.

Linke, W. A., M. Ivemeyer, P. Mundel, M. R. Stockmeier, and B. Kolmerer. 1998b. Nature of PEVK-titin elasticity in skeletal muscle. *Proc. Natl. Acad. Sci. USA.* 95:8052–8057.

Linke, W. A., M. R. Stockmeier, M. Ivemeyer, H. Hosser, and P. Mundel. 1998a. Characterizing titin's I-band Ig domain region as an entropic spring. *J. Cell Sci.* 111:1567–1574.

Lu, H., B. Isralewitz, A. Krammer, V. Vogel, and K. Schulten. 1998. Unfolding of titin immunoglobin domains by steered molecular dynamics simulation. *Biophys. J.* 75:662–671.

Oberhauser, A. F., P. E. Marszalek, H. P. Erickson, and J. M. Fernandez. 1998. The molecular elasticity of the extracellular matrix protein tenascin. *Nature.* 393:181–185.

Politou, A. S., D. J. Thomas, and A. Pastore. 1995. The folding and stability of titin immunoglobulin-like molecules with implications for mechanism of elasticity. *Biophys. J.* 69:2601–2610.

Potts, J. R., and I. D. Campbell. 1996. Structure and function of fibronectin modules. *Matrix. Biol.* 15:313–320.

Rief, M., M. Gautel, F. Oesterhelt, J. M. Fernandez, and H. E. Gaub. 1997. Reversible unfolding of individual titin immunoglobulin domains by AFM. *Science.* 276:1109–1112.

Rief, M., M. Guatel, A. Schemmel, and H. E. Gaub. 1998. The mechanical stability of immunoglobulin and fibronectin III domains in the muscle protein titin measured by atomic force microscopy. *Biophys. J.* 75: 3008–3014.

Rodiguin, N. M., and E. N. Rodiguina. 1964. Reversible-consecutive reaction. *In* Consecutive Chemical Reactions. Van Norstrand, Princeton, New Jersey. 140–167.

Trinick, J. 1996. Cytoskeleton-titin as a scaffold and spring. *Curr. Biol.* 6:258–262.

Trombitas, K., M. Greaser, S. Labeit, J. P. Jin, M. Kellermeyer, M. Helmes, and H. Granzier. 1998. Titin extensibility in situ: entropic elasticity of permanently folded and permanently unfolded molecular segments. *J. Cell Biol.* 140:853–859.

Tskhovrebova, L., and J. Trinick. 1997. Direct visualization of extensibility in isolated titin molecules. *J. Mol. Biol.* 265:100–106.

Urry, D. W. 1982. Characterization of soluble peptides of elastin by physical techniques. *Methods Enzymol.* 82:673–716.

Williamson, M. P. 1994. The structure and function of proline-rich regions in proteins. *Biochem. J.* 297:249–260.

Xu, G., and J. S. Evans. 1999. Model peptide studies of sequence repeats derived from the intracrystalline biomineralization protein, SM50. I. GVGGR and GMGGQ repeats. *Biopolymers.* 49:303–312.